ELSEVIER

Journal of Molecular Structure 520 (2000) 191–198

Journal of
MOLECULAR
STRUCTURE

www.elsevier.nl/locate/molstruc

Keto/enol tautomerism in phenylpyruvic acids: structure of the *o*-nitrophenylpyruvic acid

A.J.M. Carpy[a,*], P.P. Haasbroek[b], J. Ouhabi[a,c], D.W. Oliver[d]

[a]*Laboratoire de Physico- & Toxico-Chimie des Systèmes Naturels (LPTC), UPRES-A 5472, CNRS, Université de Bordeaux I, 351, Cours de la Libération, 33405 Talence Cedex, France*

[b]*Department of Pharmacy, Medical School, University of the Witwatersrand, 7 York Road, Parktown 2193, South Africa*

[c]*Département de Chimie, FST-Guéliz, Université Cadi Ayyad, Avenue Abdelkrim Khattabi, B.P. 618, Marrakech, Morocco*

[d]*Department of Pharmacology, Potchefstroom University for C.H.E., Potchefstroom 2520, South Africa*

Received 7 May 1999; received in revised form 2 July 1999; accepted 12 July 1999

Abstract

The synthesis of a tautomeric keto/enol mixture of *o*-nitrophenylpyruvic acid followed the acid hydrolysis of the azlactone of *o*-nitrobenzaldehyde was carried out. The structures of the two tautomeric forms were assigned by NMR spectroscopy. X-ray diffraction of a single crystal revealed that the crystalline form corresponds to the keto tautomer. Quantum mechanics calculations in the gas phase confirmed the experimental findings in solution. © 2000 Elsevier Science B.V. All rights reserved.

Keywords: Phenylpyruvic acids; Azlactones; Tautomerism; NMR; X-ray; Quantum mechanics

1. Introduction

Understanding tautomeric equilibria is of central importance in synthetic chemistry and especially in medicinal chemistry. During an investigation of the hydrolysis products (phenylpyruvic acids) of different ring-substituted aromatic azlactones, tautomerism was found to be an important aspect of phenylpyruvic acid formation [1] (Scheme 1). This study has shown that phenylpyruvic acids obtained from basic and acidic hydrolysis of these azlactones exist overwhelming in the enol form. The type and position of the substituent group in the phenyl ring of the azlactone have a definite influence on the ratio of enol/keto tautomer formation. Significant amounts of the keto tautomers could only be observed in hydrolysis products of azlactones with moderate (chlorine) or strong electron-withdrawing groups (nitro) in the *ortho*-position of the phenyl ring. Their *para*-substituted isomers formed only minute quantities of the keto tautomers, indicating that the inductive effect plays a major role in the equilibrium formation of the enol/keto tautomeric mixture when the electron-withdrawing group is in the *ortho*-position. This investigation also found that the formation of these enol tautomers and their derivatives proceed with retention of configuration of the *Z*-geometry of the parent azlactones [2–5].

Tautomerism in phenylpyruvic acids obtained from azlactones was first reported in 1943 [6]. The spectral data reported on the keto and enol forms of such acids, in some cases, seem rather confusing and inconsistent regarding tautomerism. A ^{1}H NMR spectrum of *p*-hydroxyphenylpyruvic acid in DMSO + $CDCl_3$

* Corresponding author. Tel.: + 33-556-848944; fax: + 33-556-848948.

E-mail address: a.carpy@lptc.-u-bordeaux.fr (A.J.M. Carpy).

0022-2860/00/$ - see front matter © 2000 Elsevier Science B.V. All rights reserved.
PII: S0022-2860(99)00323-3

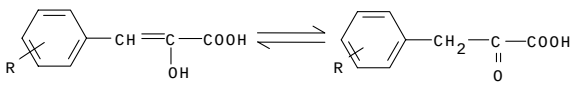

enol isomer **keto isomer**

Scheme 1.

shows only the enol form but the incorrect keto form was assigned to it [7]. The structure of the enol form of *p*-hydroxyphenylpyruvic acid was confirmed by X-ray crystallography [8]. Cyanation-hydrolysis of $PhCH_2COCl$ was reported to give 23% of the keto form of phenylpyruvic acid, whereas the synthesis from the azlactone gave the enol form [9]. More recently the formation and ^1H NMR (in DMSO) data of the enol tautomers of some ring substituted (mono-, di- and tri-substituted, mainly hydroxy and methoxy) phenylpyruvic acids synthesized from the azlactones were also reported [10]. Displacement of the keto/enol equilibrium towards the keto form can be accomplished by treating the potassium salt of the enol with H_2SO_4 (98%) in methanol [9], or in acetate buffer (pH 6) where the rate of tautomerism to the keto form is slow [8]. A ^1H NMR spectrum of *o*-nitrophenylpyruvic acid in DMSO + $CDCl_3$ shows the presence of only the keto form [7], whereas in our study the ^1H NMR and ^{13}C NMR spectra (in DMSO) of the same product obtained from the acid hydrolysis of the azlactone, clearly show the presence of the tautomeric mixture of the keto and enol forms.

This paper reports on the synthesis and NMR data of the tautomeric phenylpyruvic acid mixture obtained from the azlactone of *o*-nitrobenzaldehyde and the X-ray study performed on the keto tautomer. In addition, computational methods were used to gain information about this phenomenon and the predictability of keto/enol tautomerism as was demonstrated experimentally by the current study.

Table 1
^1H NMR data of **3a** and **3b**

Hydrogen atom	**3a** (ppm)	**3b** (ppm)
H-3 (Ar)	8.27 (dd, $J_0 = 7.9$ Hz, $J_m = 1.1$ Hz)[a]	8.15 (dd, $J_0 = 7.9$ Hz, $J_m = 1.1$ Hz)
H-4 (Ar)	7.39–7.80 (m)	7.39–7.80 (m)
H-5 (Ar)	7.39–7.80 (m)	7.39–7.80 (m)
H-6 (Ar)	7.94 (dd, $J_0 = 8.1$ Hz, $J_m = 1.1$ Hz)	7.39–7.80 (m)
Ar-CH=C	6.70 (s)	–
Ar–CH_2	–	4.65 (s)

[a] dd: double doublet; m: multiplet; s: singlet.

2. Experimental

2.1. Synthesis

The synthesis of the tautomeric mixture **3a** (enol) and **3b** (keto) involved the formation of the azlactone of *o*-nitrobenzaldehyde **2** (4-(*o*-nitrobenzylidene)-2-methyl-5-oxazolone) from *o*-nitrobenzaldehyde **1**, followed by acid (HCl/AcOH) hydrolysis. Their structures were investigated by NMR spectroscopy and X-ray crystallography. However, X-ray data could only be obtained on the keto tautomer. Difficulties in the preparation and hydrolysis of 2-nitrophenyl azlactone derivatives were reported in the literature [11,12].

2.1.1. Synthesis of azlactone of o-nitrobenzaldehyde 2

A mixture of *o*-nitrobenzaldehyde **1** (7.55 g; 0.05 mol), *N*-acetylglycine (5.85 g; 0.05 mol), anhydrous sodium acetate (8.2 g; 0.1 mol) and acetic anhydride (25 ml) was heated at 80–85°C with stirring. After 2 h, the dark brown mixture was poured into a mixture (60 ml) of equal volumes of water and ethanol, stirred for 30 min and cooled in ice. The crystals that formed were filtered off, washed with the water/ethanol mixture and dried at 45°C (4.24 g; 0.018 mol). Treatment with activated charcoal and crystallization from a mixture of benzene (4 parts) and *n*-hexane (1 part) gave yellow crystals of **2** with m.p. 115–116°C.

2.1.2. Synthesis of the tautomeric mixture of o-nitrophenylpyruvic acid 3a and 3b

The azlactone **2** (1.5 g; 6.46 mmol) was boiled under reflux with stirring in glacial acetic acid (4.5 ml) and concentrated hydrochloric acid (10.5 ml). After 6 h, the mixture was poured into water (15 ml), stirred well and cooled in a refrigerator overnight. The crystals that formed were filtered off, washed with water and dried at 45°C (0.76 g; 3.63 mmol). Recrystallization from benzene gave

Table 2
^{13}C NMR data of **3a** and **3b**

Carbon atom	**3a** (ppm)	**3b** (ppm)
*C*O–COOH	–	192.2 (s)[a]
COOH	165.8 (s)	–
CO–*C*OOH	–	162.0 (s)
C-1 (Ar)	129.7 (s)	128.5 (s)
C-2 (Ar)	148.2 (s)	148.4 (s)
C-3 (Ar)	124.9 (d)	124.2 (d)
C-4 (Ar)	132.6 (d)	131.0 (d)
C-5 (Ar)	134.1 (d)	134.1 (d)
C-6 (Ar)	128.7 (d)	127.6 (d)
Ar–CH=*C*	144.8 (s)	–
Ar–*C*H=C	102.2 (d)	–
Ar–CH_2	–	43.7 (t)

[a] s: singlet; d: doublet; t: triplet.

Table 3
Crystal data and structure refinement for **3b**

Chemical formula	$C_9H_7NO_5$
Formula weight	209.16
Crystal size (mm)	$0.32 \times 0.10 \times 0.07$
Crystal system	Monoclinic
Space group	$P2_1/c$
Unit-cell dimensions	$a = 12.765(5)$ Å, $b = 5.149(12)$ Å, $c = 14.951(3)$ Å, $\beta = 113.63(1)°$
Volume (Å^3)	900.4(1)
Z	4
Density calculated (Mg/m^3)	1.54
Absorption coefficient μ (cm^{-1})	10.6
F(000)	432
Temperature (K)	296(2)
Wavelength (Å)	1.54178
θ range for data collection	3–65°
Index ranges	$0 < h < 15$, $0 < k < 5$, $-17 < l < 16$
Unique reflections collected	1786
Observed reflections	1270
Refinement method	Full-matrix least-squares
Data/restraints/parameters	1270/0/164
Final R indices [$I \geq 3\sigma(I)$]	$R = 0.061$, $R_w^2 = 0.068$
R indices (all data)	$R = 0.077$
Largest diff. peak and hole (e Å^{-3})	0.38(8) and 0.00(8)

Table 4
Atomic coordinates ($\times 10^4$) and isotropic equivalent displacement parameter B_{eq} (Å^2) defined as: $4/3[a^2\beta_{1,1} + b^2\beta_{2,2} + c^2\beta_{3,3} + ab\cos\gamma\beta_{1,2} + ac\cos\beta\beta_{1,3} + bc\cos\alpha\beta_{2,3}]$ for **3b**

	x	y	z	B_{eq}
C(1)	6594(3)	5544(8)	1425(3)	2.21(8)
C(2)	7317(3)	3579(8)	1987(3)	2.27(8)
C(3)	7398(4)	3347(9)	2940(3)	3.0(1)
C(4)	6807(4)	4960(10)	3311(3)	3.3(1)
C(5)	6105(4)	6891(9)	2734(3)	3.2(1)
C(6)	5987(3)	7161(9)	1784(3)	2.80(9)
N(7)	6433(3)	5978(7)	404(2)	2.92(8)
O(8)	7025(3)	4817(8)	68(2)	4.90(8)
O(9)	5703(3)	7529(7)	− 81(2)	4.79(9)
C(10)	8008(3)	1789(8)	1647(3)	2.83(9)
C(11)	8981(3)	3123(8)	1526(3)	2.57(9)
O(12)	9399(3)	5148(6)	1914(2)	3.58(7)
C(13)	9480(3)	1762(8)	871(3)	2.70(9)
O(14)	9009(3)	− 166(6)	413(2)	3.83(7)
O(15)	10390(3)	2833(6)	854(2)	4.02(7)

cream-colored crystals of **3a** and **3b** with m.p. 120–122°C.

2.2. Spectroscopic analysis

NMR analysis of the tautomeric mixture, **3a** and **3b**, was performed at 200 MHz (^{1}H) and 50 MHz (^{13}C) on a Bruker AC-200 spectrometer with DMSO-d_6 as solvent and TMS as internal standard (Tables 1 and 2). The melting points (uncorrected) were determined on an electrothermal melting point apparatus.

2.3. X-ray analysis

A pale yellow crystal (dimensions $0.32 \times 0.10 \times 0.07$ mm) was mounted on an Enraf-Nonius CAD-4 diffractometer using graphite-monochromated Cu K_α radiation. The crystal data are listed in Table 3. Lattice parameters were determined by least-squares refinement of 25 reflections with $20° < \theta < 35°$. Intensities were collected with $\omega - 2\theta$ scan mode, up to $\theta = 65°$. The intensities of two standard reflections, measured every 90 min, showed no significant deviation. The data were corrected for Lorentz and polarization effects but not for absorption ($\mu = 10.6$ cm^{-1}). A total of 1786 unique reflections were collected, of which 1270 with $I \geq 3\sigma(I)$ were considered as observed. The structure was solved by

Table 5
Bond lengths (Å) for **3b**

	RX	AMPAC-AM1	RHF/6-31G	RHF/6-31G**	B3LYP/6-31G**
C(1)–C(2)	1.399(5)	1.409	1.398	1.396	1.408
C(1)–C(6)	1.385(7)	1.407	1.388	1.385	1.397
C(1)–N(7)	1.473(5)	1.490	1.450	1.460	1.473
C(2)–C(3)	1.391(6)	1.402	1.391	1.389	1.400
C(2)–C(10)	1.498(7)	1.488	1.512	1.512	1.508
C(3)–C(4)	1.381(7)	1.392	1.385	1.384	1.393
C(4)–C(5)	1.382(6)	1.394	1.386	1.384	1.395
C(5)–C(6)	1.375(6)	1.391	1.381	1.380	1.389
N(7)–O(8)	1.219(6)	1.202	1.231	1.198	1.236
N(7)–O(9)	1.221(5)	1.201	1.223	1.191	1.229
C(10)–C(11)	1.493(7)	1.501	1.510	1.517	1.526
C(11)–O(12)	1.208(5)	1.225	1.207	1.183	1.208
C(11)–C(13)	1.536(7)	1.509	1.511	1.532	1.543
C(13)–O(14)	1.219(5)	1.233	1.210	1.187	1.212
C(13)–O(15)	1.295(6)	1.354	1.332	1.312	1.339

direct methods using MolEN [13] and refined anisotropically. It was determined that the crystal corresponded to the **3b** keto form. The final residuals were $R = 0.061$ ($R_w = 0.068$). The final fractional coordinates for **3b** and equivalent displacement parameters are listed in Table 4. The bond lengths and angles are given in Tables 5 and 6. The selected torsion angles are shown in Table 7.

2.4. Computational analysis

Semi-empirical calculations, geometry optimizations and frequency calculations, were performed on **3b** and **3a** with the AMPAC 6.0 package [14] and the AM1 Hamiltonian. The corresponding ab initio calculations were carried out by using the GAUSSIAN94 program package [15] at Hartree–Fock (RHF) (6-31G and

Table 6
Bond angles (°) for **3b**

	RX	AMPAC-AM1	RHF/6-31G	RHF/6-31G**	B3LYP/6-31G**
C(2)–C(1)–C(6)	122.6(4)	120.7	122.3	122.5	122.3
C(2)–C(1)–N(7)	121.1(4)	122.0	121.4	121.3	121.6
C(6)–C(1)–N(7)	116.3(3)	117.3	116.3	116.1	116.0
C(1)–C(2)–C(3)	116.0(4)	118.1	116.6	116.4	116.3
C(1)–C(2)–C(10)	125.2(4)	123.7	124.7	124.8	124.6
C(3)–C(2)–C(10)	118.8(3)	118.2	118.8	118.8	119.1
C(2)–C(3)–C(4)	122.1(4)	121.2	121.8	121.9	122.1
C(3)–C(4)–C(5)	120.2(4)	120.1	120.3	120.3	120.1
C(4)–C(5)–C(6)	119.5(5)	120.0	119.3	119.3	119.4
C(1)–C(6)–C(5)	119.6(4)	119.8	119.7	119.6	119.7
C(1)–N(7)–O(8)	120.0(3)	119.9	119.0	118.4	118.7
C(1)–N(7)–O(9)	118.0(4)	118.3	118.4	117.7	117.8
O(8)–N(7)–O(9)	121.9(4)	121.7	122.6	123.9	123.5
C(2)–C(10)–C(11)	112.9(4)	113.7	112.5	112.3	112.7
C(10)–C(11)–O(12)	124.6(4)	126.3	123.6	124.3	124.4
C(10)–C(11)–C(13)	116.5(4)	112.4	115.6	115.1	114.3
O(12)–C(11)–C(13)	118.9(4)	121.3	120.7	120.5	121.2
C(11)–C(13)–O(14)	119.5(4)	127.2	122.1	122.1	123.0
C(11)–C(13)–O(15)	115.0(4)	114.6	113.9	113.1	112.2
O(14)–C(13)–O(15)	125.4(5)	118.2	123.9	124.9	124.7

Table 7
Selected torsion angles (°) for **3b**

	RX	AMPAC-AM1	RHF/6-31G	RHF/6-31G**	B3LYP/6-31G**
O(9)–N(7)–C(1)–C(6)	− 7.1(6)	18.5	− 16.7	− 19.6	− 14.3
C(3)–C(2)–C(10)–C(11)	− 108.2(4)	− 108.7	− 106.2	− 103.9	− 107.2
C(2)–C(10)–C(11)–C(13)	− 160.0(3)	161.2	− 151.2	− 154.2	− 154.7
C(10)–C(11)–C(13)–O(15)	− 173.7(3)	122.9	167.8	165.7	173.5

6-31G** basis sets) and density functional (DF) (B3LYP/6-31G** [16,17]) levels. The geometries were optimized using Berny's algorithm [18]. Following the geometry optimizations, analytical frequency calculations were carried out at the RHF/6-31G level only, using standard procedures [19], to obtain thermochemical properties. The tautomeric keto ⇔ enol equilibrium in the phenylpyruvic acid was presented in Scheme 1.

The ratio of the two tautomers is described by the equilibrium constant K_T, which is classically calculated from their free energy difference ΔG

$$K_T = \exp(-\Delta G/RT) \quad (1)$$

ΔG is expressed as a function of enthalpy difference ΔH and entropy difference ΔS

$$\Delta G = \Delta H - T\Delta S \quad (2)$$

The enthalpy difference ΔH at 298 K is given by

$$\Delta H^{298} = \Delta E_T + \Delta E_v^0 + \Delta(\Delta E_v^{298}) + \Delta E_r^{298} + \Delta E_t^{298} + \Delta(PV) \quad (3)$$

where E_T is the total energy, E_v^0 the zero-point energy (ZPE), ΔE_v^{298} the change in vibrational energy when T increases from 0 to 298.15 K, E_r^{298} and E_t^{298} are the rotational and translational energies, and PV is the work term. In the tautomeric equilibria, the last three terms of Eq. (3) are all zero. For comparison, the same calculations were performed on the phenylpyruvic acid itself and on the *o*-chloro substituted compound.

3. Results and discussion

3.1. Spectroscopic analysis

The ^{1}H NMR data of **3a** and **3b** are given in Table 1. Investigation of the ^{1}H NMR spectrum of the hydrolysis product of the azlactone of *o*-nitrobenzaldehyde revealed the presence of a mixture of the enol **3a** and keto **3b** tautomers of *o*-nitrophenylpyruvic acid. The signal at 6.70 ppm accounts for the single benzylic proton of the enol tautomer, and the signal at 4.65 ppm for the two benzylic protons of the keto tautomer. Peak intensity calculations show that this tautomeric mixture consists of approximately 59% of the enol form and 41% of the keto form.

The ^{13}C NMR data of **3a** and **3b** are given in Table 2. Two sets of chemical shift values could clearly be distinguished for the two tautomeric forms. The signal at 144.8 ppm (α-carbon, Ar-CH=*C*), and the signal at 102.2 ppm (benzylic carbon, Ar-*C*H=C) are evidence for the presence of the enol tautomer **3a**. These values are in accordance with values that have already been observed for other enol tautomer derivatives [1,2,8,10]. The low field signal at 192.2 ppm was assigned to the carbon atom of the α-carbonyl group (−*C*O−COOH) and the high field signal at 43.7 ppm (triplet) to the benzylic carbon (Ar−*C*H$_2$) of the keto tautomer **3b**. These chemical shift values were found to be characteristic of the keto form and represent therefore a unique and effective way to identify the presence of the keto form, even in trace amounts [1].

3.2. Structure assignment of *3b* by X-ray diffraction

The keto structure of **3b** was established by X-ray diffraction on a single crystal. An ORTEP view of two molecules paired by H-bonds involving the carboxylic acid groups, and showing the atomic numbering is depicted in Fig. 1. Bond lengths between C(11) and C(10) (1.493(7) Å) and between C(11) and O(12) (1.208(5) Å) clearly indicate that the selected crystal existed with the keto form. The orientation of the trans-extended side chain (including the acid moiety) towards the phenyl ring is defined by the value of the

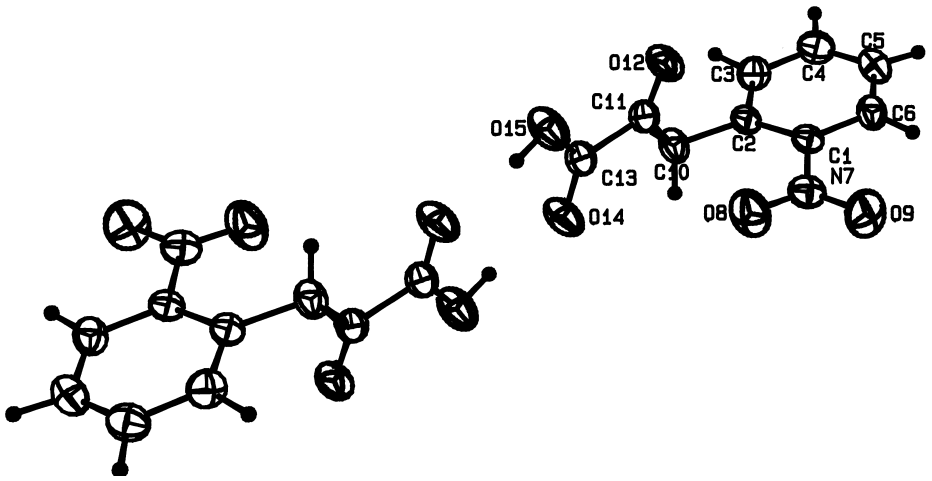

Fig. 1. ORTEP view of a pair of **3b** molecules linked by H-bonds.

torsion angle C(3)–C(2)–C(10)–C(11) = −108.2(4)° (Table 7). The dihedral angle between the phenyl ring and the plane containing the keto group [C–C(=O)–C] is equal to 80.3(1)°. The *o*-nitro group is nearly coplanar with the aromatic ring with a torsion angle O(9)–N(7)–C(1)–C(6) = −7.1(6)°.

3.3. Computational analysis

The geometries of the two tautomeric forms were optimized using AMPAC-AM1 and GAUSSIAN94 at Hartree–Fock (basis sets 6-31G and 6-31G**) and density functional (B3LYP/-631G**) levels. Only the geometry of **3b**, calculated with these methods, is reported in Tables 5–7 for comparison with experimental results. Although it is trivial to notice that ab initio calculations reproduced the geometry better than the semi-empirical method, the advantages of AMPAC (diffusion of the program, computational time, etc.) have to be considered. Except RHF/6-31G**, the other three methods tend to overestimate bond lengths. It is particularly true for B3LYP/6-31G** which overestimate 12 of the 15 bond lengths. However, the average difference between bond lengths calculated with this method and experimental ones is only 0.013 Å, intermediate between RHF/6-31G results (0.011 Å) and RHF/6-31G** results (0.015 Å). The same data, calculated with AMPAC, is 0.018 Å. For all methods, the highest individual differences between experimental and calculated bond lengths are found in the terminal carboxylic group (H-bonds are not considered in the calculations) (Table 5). The calculated bond angles are statistically over- and underestimated. The average difference between experimental and calculated bond angles are 1.7° (AMPAC-AM1), 0.6° (RHF/6-31G and 6-31G**) and 0.9° (B3LYP/6-31G**). At the Hartree–Fock level, this difference is very close to the average s.d. of experimental bond angles (0.4°) (Table 6). Finally, the *trans* extended conformation

Table 8
Total energies and total energy differences (entropies and zero-point energy (ZPE) plus thermal corrections)

	E (a.u.)		Δ*E* (kcal mol^{-1})	Entropy (cal mol^{-1} K^{-1})		ZPE + thermal correct (kcal mol^{-1})	
	Keto form	Enol form	Keto − enol	Keto form	Enol form	Keto form	Enol form
Phenylpyruvic acid	569.82230	− 569.83287	6.63	105.795	98.075	110.038	110.558
o-Nitro derivative	− 773.17193	− 773.17034	− 1.00	113.075	100.962	113.470	112.630
o-Chloro derivative	− 1028.69901	− 1028.70682	4.89	108.809	105.547	104.545	105.039

Table 9
Tautomer equilibrium constant K_T of the reaction keto form ↔ enol form

	ΔH (kcal mol^{-1})	ΔG (kcal mol^{-1})	K_T
Phenylpyruvic acid	− 6.11	− 3.81	624.8
o-Nitro derivative	0.16	3.77	1.73×10^{-3}
o-Chloro derivative	− 4.40	− 3.43	326.8

of the side chain is only reproduced by the ab initio methods. AMPAC tilted the nitro group from the phenyl ring by an angle almost equal in value, but opposite in sign, to the angle found by the ab initio methods; the torsion angle defining the position of the OH group of the carboxy moiety is closest to 90° (122.9°) than to 180° (*trans* extended as found in the crystals and by ab initio calculations).

According to these results, the analytical frequency and thermodynamic calculations were only performed with the RHF/6-31G method. For comparison, the same calculations were also performed on the phenylpyruvic acid itself, on the *o*-nitrophenylpyruvic acid and on the *o*-chlorophenylpyruvic acid. The total energies and the total energy differences between the two tautomeric forms [ΔE(keto − enol)] are listed in Table 8. The enol forms of phenylpyruvic acid and of the *o*-chloro derivative are more stable than the keto forms as previously observed [1]. The energy differences for phenylpyruvic acid and the *o*-chloro derivative are, respectively, around 6.63 and 4.89 kcal mol^{-1}. However, the energy difference between the **3b** (keto form) and **3a** (enol form) favored the more stable keto form by 1 kcal mol^{-1}.

Values of entropies and ZPE plus thermal corrections at $T = 298$ K are listed in Table 8. From Eqs. (1)–(3) and the values extracted from Tables 8 and 9, the tautomeric equilibrium constants could be calculated. The calculations show a large preference for the enol tautomers relative to the keto tautomers in the case of the non-substituted- and the *o*-chloro-substituted molecules ($K_T > 1$). Conversely, the tautomeric constant K_T of the equilibrium **3b** ↔ **3a** is equal to 1.73×10^{-3} showing a large preference for **3b** ($K_T^{-1} = 579.3$).

4. Conclusion

The synthesis of a tautomeric keto/enol mixture (**3b/3a**) of *o*-nitrophenylpyruvic acid resulted from the acid hydrolysis of the azlactone of *o*-nitrobenzaldehyde. The structures of the two forms were identified by NMR spectroscopy. Their proportions in the mixture were based on the peak intensities of the ^{1}H NMR spectra of **3a** and **3b**. Approximately 59% of the enol form and 41% of the keto form are present in the mixture in DMSO at room temperature. Increasing the temperature of this mixture increased the percentage of the keto form. Subsequent NMR studies have shown that the keto/enol ratios are solvent and temperature dependent [1,20].

Following the crystallization process, only the keto form **3b** crystallized. Its structure was unambiguously determined by X-ray crystallography.

The phenylpyruvic acids synthesized from the corresponding azlactones, favored their existence in the enol form, in the unsubstituted as well as in different substituted phenylpyruvic acids and only electron-withdrawing groups in the *ortho* position of the phenyl ring causes displacement of the equilibrium towards keto formation [1–5]. The tautomeric equilibrium was investigated in the gas phase by quantum mechanics calculations. Three potential keto/enol mixtures were investigated: the phenylpyruvic acid itself, the *o*-nitrophenylpyruvic acid and the *o*-chlorophenylpyruvic acid. Ab initio calculations showed that the unsubstituted acid exists predominantly in the enol form confirming our experimental findings. The strong electron-withdrawing nitro group in the *ortho* position has a significant influence on the formation of the keto/enol tautomeric mixture, by shifting the equilibrium towards keto formation. As expected, the chlorine atom in the *ortho* position being a moderate electron-withdrawing group had a lesser influence than the nitro group. Consequently the equilibrium is still in favor of the enol form as found experimentally (∼88% of the enol tautomer and 12% of the keto tautomer are present in DMSO at room temperature) [1]. In conclusion, this

study has shown that substitution type and substitution position clearly play an important role in the keto/enol tautomerism of phenylpyruvic acid derivatives.

References

[1] P.P. Haasbroek, Ph.D. Thesis, Potchefstroom University for C.H.E., Potchefstroom, South Africa, 1997.
[2] D.W. Oliver, P.P. Haasbroek, J.M. Leger, A.J.M. Carpy, J. Chem. Crystallogr. 24 (1994) 665.
[3] P.P. Haasbroek, D.W. Oliver, A.J.M. Carpy, J. Chem. Crystallogr. 28 (1998) 139.
[4] P.P. Haasbroek, D.W. Oliver, A.J.M. Carpy, J. Chem. Crystallogr. 28 (1998) 193.
[5] P.P. Haasbroek, D.W. Oliver, A.J.M. Carpy, J. Chem. Crystallogr. 28 (1998) 811.
[6] L.C. Raiford, C.H. Buurman, J. Org. Chem. 8 (1943) 466.
[7] C.J. Pouchert, J.R. Campbell, The Aldrich Library of NMR Spectra, VI, Aldrich Chemical Company, 1974, p. 127.
[8] M.C. Pirrung, J. Chen, E.G. Rowley, A.T. McPhail, J. Am. Chem. Soc. 115 (1993) 7103.
[9] I.J. Pérez, S.M. Rosell, Afinidad 36 (1979) 332.
[10] H.N.C. Wong, Z.L. Xu, H.M. Chang, C.M. Lee, Synthesis 8 (1992) 793.
[11] J.M. Gulland, K.I. Ross, N.B. Smellie, J. Chem. Soc. (1931) 2885.
[12] H. Burton, J. Chem. Soc. (1935) 1265.
[13] MolEN, An Interactive Structure Solution Procedure, Enraf-Nonius, Delft, The Netherlands, 1990.
[14] AMPAC 6.0, Semichem, 7128 Summit, Shawnee, KS 66216, USA.
[15] M.J. Frisch, G.W. Trucks, H.B. Schlegel, P.M.W. Gill, B.G. Johnson, M.A. Robb, J.R. Cheeseman, T. Keith, G.A. Peterson, J.A. Montgomery, K. Raghavachari, M.A. Al-Laham, V.G. Zakrewski, J.V. Ortiz, J.B. Foresman, C.Y. Peng, P.Y. Ayala, W. Chen, M.W. Wong, J.L. Andres, E.S. Replogle, R. Gomperts, R.L. Martin, D.J. Fox, J.S. Binkley, D.J. Defrees, J. Baker, J.P. Stewart, M. Head-Gordon, C. Gonzalez, J.A. Pople, GAUSSIAN94, revision B.3, Gaussian, Inc., Pittsburgh, PA, 1995.
[16] R.G. Parr, W. Yang, Density-Functional Theory of Atoms and Molecules, Oxford University Press, Oxford, 1989.
[17] A.D. Becke, J. Chem. Phys. 98 (1993) 5648.
[18] H.B. Schlegel, J. Comput. Chem. 3 (1982) 214.
[19] W.J. Hehre, L. Radom, P.v.R. Schleyer, J.A. Pople, Ab Initio Molecular Orbital Theory, Wiley, New York, 1986, chap. 6.
[20] Details to be published elsewhere.